American Journal of Physics and Applications
2015; 3(4): 121-130
Published online July 1, 2015 (http://www.sciencepublishinggroup.com/j/ajpa)
doi: 10.11648/j.ajpa.20150304.12
ISSN: 2330-4286 (Print); ISSN: 2330-4308 (Online)

On the Mathematical Calibration of the Active Well Neutron Coincidence Counter (AWCC)

Wael A. El-Gammal[1], Ahmed G. Mostafa[2], Mootaz Ebied[3]

[1]Egyptian Nuclear and Radiological Regulatory Authority, Division of Regulations and Radiological Emergencies, Department of Nuclear Safeguards and Physical Protection, Cairo, Egypt
[2]Faculty of Science, Physics Department, Al-Azhar Univ., Cairo, Egypt
[3]Atomic Energy Authority, National Center for Radiation Research and Technology, Division of Industrial Irradiation, Department of Nuclear Safety Research and Radiation Emergency, Cairo, Egypt

Email address:
wgammal66@yahoo.com (W. A. El-Gammal)

To cite this article:
Wael A. El-Gammal, Ahmed G. Mostafa, Mootaz Ebied. On the Mathematical Calibration of the Active Well Neutron Coincidence Counter (AWCC). *American Journal of Physics and Applications*. Vol. 3, No. 4, 2015, pp. 121-130. doi: 10.11648/j.ajpa.20150304.12

Abstract: Generation of calibration curves for radiation detectors are essential in radiation spectroscopy. Such curves usually relate some characteristic quantities of measured samples (such as radioactivity of a certain isotope or its mass) with the output of the used detector (counting rates). The most direct and easiest way to generate these curves is performed using a set of suitable radioactive standard materials. Whenever standard materials are not available, mathematical calibration could be employed. In this work, a proposed model for mathematical calibration of a neutron coincidence counter (the Active Well Neutron Coincidence Counter, AWCC) was achieved using the Monte Carlo simulation method. Effects of the counter and experimental set up parameters on the simulation process were studied. The validity of the proposed model was checked using sets of nuclear material standards. The obtained modeling results are in agreement with experiments within an accuracy of better than 8.5%.

Keywords: Nuclear Safeguards, Monte Carlo, Mathematical Calibration, Uranium, AWCC

1. Introduction

In the field of nuclear safeguards, the Active Well Coincidence Counter (AWCC) Figure (1) is one of the main devices that are used to verify Nuclear Materials (NMs). The AWCC is a neutron coincidence counting system [1]. It is a transportable high-efficiency counter for measuring uranium isotopic masses in uranium bearing materials. The active mode operation of the AWCC is based on the detection of coincidence neutrons produced from induced fission of ^{235}U isotope using interrogation neutron sources (one or more Am-Li neutron sources are inserted in the top and/or bottom of the detector well). The AWCC construction and operation was described and explained by different authors in many papers and technical reports [1-5].

Calibration of the AWCC (^{235}U mass versus coincidence counts) normally performed through measuring standard NM samples. Because of neutron absorption and multiplication in uranium samples, the calibration curves are nonlinear and are sensitive to the geometry, ^{235}U density and other factors. Therefore, to obtain accurate results, the assayed samples must be very similar to the standards used for calibration. However, an appropriate calibration curve is not always available, either because suitable standards are not available or because the characteristics of the assayed samples are not well known [6].

The AWCC was tested and used in different applications by many authors [7-17]. It was compared with other neutron coincidence detectors to investigate its precision, counting rate, accuracy, stability, and the effect of sample inhomogeneity [7, 8]. Menlove and Bosler [9] showed that the instrument could be used for assaying wide range of HEU samples in form of stacked disks to simulate buttons and thin metal plates both in thermal and fast modes taking into consideration the neutron self-shielding and multiplication. The AWCC was also calibrated [10] for assaying 93%-enriched fuel materials in different categories. Evaluation of the AWCC for field tests was performed by

Krick and Rinard [11]. They demonstrated its applicability for assaying the uranium content of a wide variety of materials and generated calibration curves for different NM categories. A semi-empirical calibration formula to calibrate the AWCC for ^{235}U measurements was developed by El-Gammal et al. and Winn et al. [1, 12]. The AWCC was also used for assaying HEU samples with variation in matrix impurity [13], characterization of unknown NM samples [14], and cross-calibration investigation and other applications [15-17]. Rinard and Menlove [18] used the MCNP–REN code to model the AWCC in a configuration used to measure the uranium linear density in long fuel elements. The simulation results showed about 10% positive bias. Pozzi et al [19] used MCNP-PoliMi code to simulate the measurements performed with AWCC via simulating the operation of the counter shift register. They showed that the calculated efficiency for the AWCC using Cf-252 is 29% while in case of induced fission neutron detection, the efficiency reduced to be 25.6% using 6.0 kg of uranium metal with 92.0% enrichment and with Am Li neutron sources in their positions.

In most of the reviewed work, it was noticed that to obtain accurate quantitative measurements, it is necessary to calibrate the instrument using physical standards representing the samples to be assayed. Almost, the availability of such standards with different forms and categories covering the assayed NM in field is not available. In this work a model for AWCC calibration is proposed. The model employs the MC method using the general MCNP5 code.

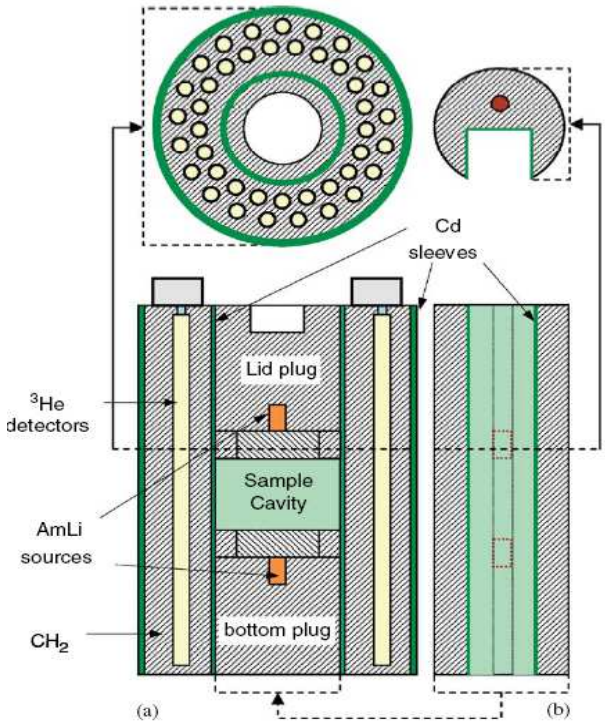

Fig. (1). *Schematic diagram of the AWCC, (a) main components and (b) the MTR insert [1].*

2. Methodology

Neutrons can be emitted from isotopes in three ways: (1) spontaneous fission, (2) induced fission, and (3) α particle-induced reactions, (α, n) [20]. Fission neutrons are emitted in groups of two or more for each fission event. The number of neutrons emitted in spontaneous or induced fission is called the neutron multiplicity (ν). This signature could be detected as a neutron coincidence. [21].

The operation of the AWCC is based on the detection of timely correlated spontaneous (fast mode) or induced (thermal mode) fission neutrons. The relation between the mass content of uranium isotope and the total measured real coincidence count rate (Cr, s-1) might take the form:

$$Cr = \sum_x Cr_x = \sum_x M_x F_x f_{cx} \quad (1)$$

Where,

Cr_x is the real coincidence count rate due to isotope $\boldsymbol{x}$ (s^{-1}),

M_x is the mass of isotope $\boldsymbol{x}$ (g),

F_x is the total specific fission rate of isotope $\boldsymbol{x}$ (fissions/s.g), and

f_{cx} is the counter coincidence counting efficiency due to the fission neutrons of isotope $\boldsymbol{x}$.

Eq. (1) indicates that the real coincidence count rate measured by AWCC is a function of the physical properties of the assayed sample, fission rate and coincidence counting efficiency of the detector. The sample physical properties include mass content of isotope *x*, type of matrix material, density, dimensions and other properties for the container.

In the active thermal mode operation of the AWCC, the value of the specific fission rate F_x equals to the sum of three components which are the spontaneous fission rate, induced fission rate due to external interrogation neutron sources, and self-induced fission rate, per gram isotope.

The spontaneous fission yields of the uranium isotopes (^{234}U, ^{235}U and ^{238}U) are of negligible values in comparison with the ^{235}U induced fission yield. [21]. On the other hand, the probability of interaction between thermal neutrons from induced fission with other uranium nuclei (^{234}U or ^{238}U) to produce additional fissions is very low (fission cross-section less than 10 barns) [22]. Therefore, for low enriched and small mass uranium samples assayed in thermal mode, the coincidence neutrons due to (1) induced fissions by fast neutrons from Am Li interrogation sources, (2) spontaneous fissions and (3) self-induced fissions, could affect the measurements with ignorable values. The ^{238}U fission rate contributions in active-thermal mode operation for AWCC are only less than 0.6% and 0.3% from the total fission rate of DU and NU samples respectively [23].

Hence, coincidence counts due to interactions of the thermalized AmLi neutrons with ^{235}U nuclei are dominated. Consequently, Eq. (1) could be rewritten as:

$$Cr \cong Cr_5 = M_5 F_5 f_{c5} \quad (2)$$

The process of neutron detection in the AWCC device starts when neutrons emitted from the interrogation neutron sources (AmLi sources). These neutrons emitted with a certain spectrum and are thermalized in the polyethylene detector body. Because of the thermalization process, thermal neutrons with a new energy spectrum will start interacting with fissile isotopes of the NM sample in the cavity of the detector. Among all types of reactions, fission reaction will take place with a specific fission rate depending on many parameters that may include neutron spectrum, counter material and configuration, full characteristics of the measured sample and its location inside the cavity. Induced fission neutrons interact, with a certain probability, with the helium detectors of the counter (as singles). If the neutrons are detected within a specific period of time they are assigned as coincidence ones and indicates a fission. Therefore, neutrons counted in the detector are given as singles and when treated (correlated with respect to time) they are given as coincidence. Finally, the coincidence count rate given by the counter is a function of the mass of the isotope in the assayed sample. The effect of all parameters described in the detection process must be taken into consideration while calibrating the detector. To avoid estimating the effect of such parameters and simultaneously to overcome the lack of NM standards, a model has been suggested to calibrate the detector mathematically. A full mathematical calibration of the AWCC will take into account the fission rate and counter efficiency indicated in Eqn. (2). For a uranium-bearing sample assayed in the AWCC, the coincidence count rate could be given as:

$$C_{r5} \cong C_r = \left(\frac{S_T - S_O}{\nu_T}\right) \cdot \left(1 - \frac{S_f}{f_t}\right) \tag{3}$$

Where:

C_{r5} is the real coincidence count rate due to ^{235}U isotope (s^{-1}).

S_T is the total singles count rate (s^{-1}), estimated using MC calculations.

S_o is the total singles count rate (s^{-1}) due to all interactions but fission, estimated using MC calculations for samples free of any NM.

S_f is the singles count rate for fission neutrons with ν=1 (s^{-1}).

S_f/f_t is the fraction of the fission neutrons (with ν=1) to the total fission neutrons (it could be deduced from induced fission multiplicity table from the MCNPX output file).

ν_T is the total neutron multiplicity for the mean value of neutrons emitted per spontaneous or induced fission (it could be deduced from induced fission multiplicity table from the MCNPX output file for every correspondence single or couple measured samples).

3. Experimental Setup and Technique

3.1. System Setup

The used AWCC system [Canberra, Model JCC-51] consists of a high-density polyethylene ring in which 42 ^3He thermal-neutron detectors [Reuter-Stokes model RS-P40820-103] are imbedded into polyethylene in a cylindrical arrangement around a central sample cavity. The detectors are wired to give six groups of seven tubes for each. Each group is ganged through a single preamplifier/ amplifier/ discriminator board [JAB-01 Amptek]. The board output pulses are analyzed by the neutron analysis shift register [model JSR-14] with the detector parameters shown in Table (1). The system uses two $^{241}AmO_2$–Li neutron sources (Gammatron, model AN-HP) above and below with yields of 4.45×10^4 n/s of each, giving combined source strength of $8.9x10^4$ n/s to activate thermal fission in assayed samples. The yield was calculated from the initial certified yield and depending on the data given by Tagziria and Looman (2012) [24]. Each source is kept in a stainless-steel container. A tungsten shield is placed around each source to reduce the γ-ray emission [25-27].

Table 1. *Detector parameters and timing characteristics used for this work.*

Gate width	Pre-delay time	High voltage	Die-away time
64 μs	4.5 μs	1680 V	52.36 μs

The counter was used in the vertical configuration, active thermal mode, with 27.54 cm cavity space and 22.86 cm diameter. The AmLi sources were placed at their positions in lower and lid plugs, at 10.72 cm and 42.74 cm from the bottom of the detector to allow optimum sample interrogation. The measuring setup parameters for data acquisition are adjusted using Canberra JSR-14 neutron coincidence software.

3.2. Measured Samples

Two identical sets of standard nuclear material (SNM) samples "NBS-SRM-969" were used in the measurements (IDs: NBS-111 & NBS-128). Every set consists of five sealed samples in addition to an empty unsealed can [28]. Detailed information on each sample is shown in Table (2). The cans are made from aluminum type 6061 (ASTM-GS T6) and containing 200.1 g of uranium oxide U_3O_8. The outer can diameter is 80 mm, the internal diameter of the can is 70.0 mm and the height is 89 mm.

The base has a well specified thickness of 2.00 mm. The fill height, according to the degree of compression applied to the powder, for all samples is (20.8±0.5) mm except for sample SRM969-446 for which the height is (15.8±0.5) mm. Figure (2) shows the NBS-SRM-969 set [29].

Table 2. *Description of the SNM samples (NBS-SRM-969) used in the measurements.*

Sample ID		Fill Height (cm)	Density (g/cm^3)	Certified/declared values of uranium				
				U_3O_8 Weight (g)	^{235}U Weight (g)	Reference relative abundance		
						^{235}U (atom %)	^{238}U (atom %)	^{234}U (atom %)
SRM969-031	NBS-111 NBS-128	2.08 ± 0.05	2.50±0.06	200.1 ± 0.2	0.5260	0.3206±0.0002	99.6627±0.0004	0.0020±0.0002
SRM969-071	NBS-111 NBS-128	2.08 ± 0.05	2.50±0.06	200.1 ± 0.2	1.2047	0.7209±0.0005	99.2738±0.0004	0.0053±0.0002
SRM969-194	NBS-111 NBS-128	2.08 ± 0.05	2.50±0.06	200.1 ± 0.2	3.2918	1.9664±0.0014	98.0159±0.0018	0.0174±0.0002
SRM969-295	NBS-111 NBS-128	2.08 ± 0.05	2.50±0.06	200.1 ± 0.2	5.0056	2.9857±0.0021	96.9826±0.0029	0.0284±0.0004
SRM969-446	NBS-111 NBS-128	1.58 ± 0.05	3.291±0.1	200.1 ± 0.2	7.5678	4.5168±0.0032	95.4398±0.0032	0.0365±0.0003

Fig. (2). *Photograph of the NBS-SRM-969 standards. The empty can is shown disassembled and the plunger in the foreground without the ultrasonic seal, [29].*

3.3. NM Measurements

Real coincidence count rates (C_{r5}) for four of the SNM samples (SRM969-071, 194, 295 and 446) measured as single samples covering a small range of ^{235}U masses (from 1.2 g to 7.5 g, Table (4). The outer shell of the empty unsealed aluminum can was used as a holder for these singles samples from the bottom of the detector. To increase the range of ^{235}U masses, the SNM samples were measured as couples. The chosen eight couples for coupling to cover a range of ^{235}U masses extends from 2.4 g to 15.1 g are shown in Table (5).

The measurement locations inside the cavity are illustrated in Figure (3). Three runs were taken for every single sample or couple measurements for a live time of 7.5 hours each. The uncertainty for the measured Cr5 for singles varies between 1.2% and 0.5% RSD and varies between 0.7% and 0.16% RSD for couples. The measured C_{r5} were then compared with those calculated using the MCNP code according to Eqn. (3).

3.4. Monte Carlo Modeling for AWCC

The characteristics and specifications of the AWCC components, SNM, holder and containers were modeled with as much detail as possible in order to reflect as much of the experimental setup as possible, Figure (3).

The instrument dimensions, its components, their locations, effective lengths, densities, material properties of ^{3}He and AmLi sources yields and orientation were obtained or calculated according to the available data given in different references [2, 3, 25, 26, 30 and 31]. The ideal $^{241}AmLi$ neutron source energy spectrum, in a numerical format, used in the simulation process was calculated by Tagziria and Looman [24].

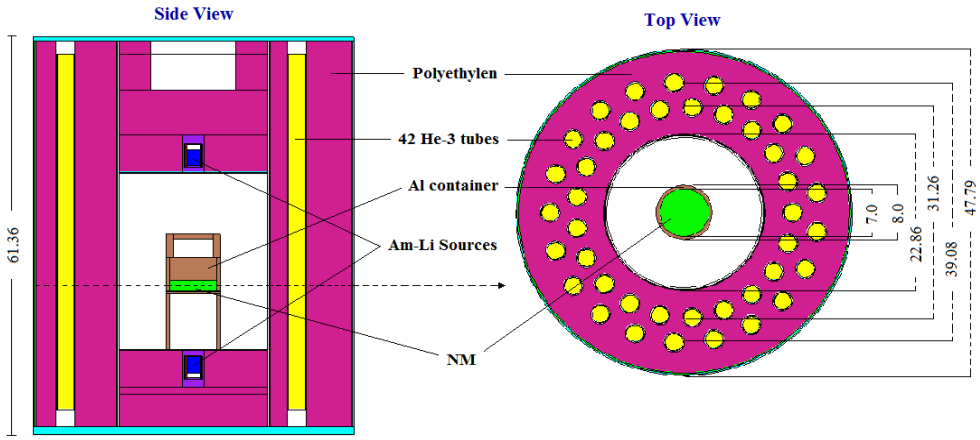

Fig. (3). *MCNP model of the Canberra JCC-51 Active Well Coincidence Counter.*

The total singles count rate detected in ^{3}He were tallied using the track length estimate of cell flux (F4: N n_i) with the tally multiplier card (FM4 C M R_1), where N means that MCNP code is running in a neutron transport mode, ni is the cells numbers for all the 42 cell that contain ^{3}He gas, C is the atomic density of the material (^{3}He gas), M is the material number on material card, and (R_1=103) is the reaction number for (n, p) reaction [32], where the neutron is converted inside the ^{3}He tubes through the following nuclear reaction to be proton which could be counted:

$$ {}_0^1n + {}_2^3He \rightarrow {}_1^3H + {}_1^1H + 0.764MeV $$

553 MCNP input files were designed to perform the calculations. Each calculational run was performed using 5x106 histories for about 30 minutes on a 2.5 GHz Intel Core i5 processor. The relative standard deviation did not exceed 0.15% for all runs. The calculations were performed without using any variance reduction technique. The tally results are normalized to be per starting particle and the total singles count rate, could be determined based on the total yield of AmLi sources, which has been calculated at the time of practical measurements.

3.5 The Sources of Error Affecting the MC Modeling

The main source of errors depends on the accuracy of information obtained from literature or incomplete data provided by the manufacturer for the AWCC components. All factors that were expected to contribute to the overall errors were studied. These include the Al container and holder effects, for which the calculations were repeated for different setup configurations (different parts of Al can and the holder were removed) for both the singles and couples cases. Figure (4), shows the removed parts. As shown in Figure (4.a), the removed parts are (I) the Al container, (II) the plunger and (III) the holder.

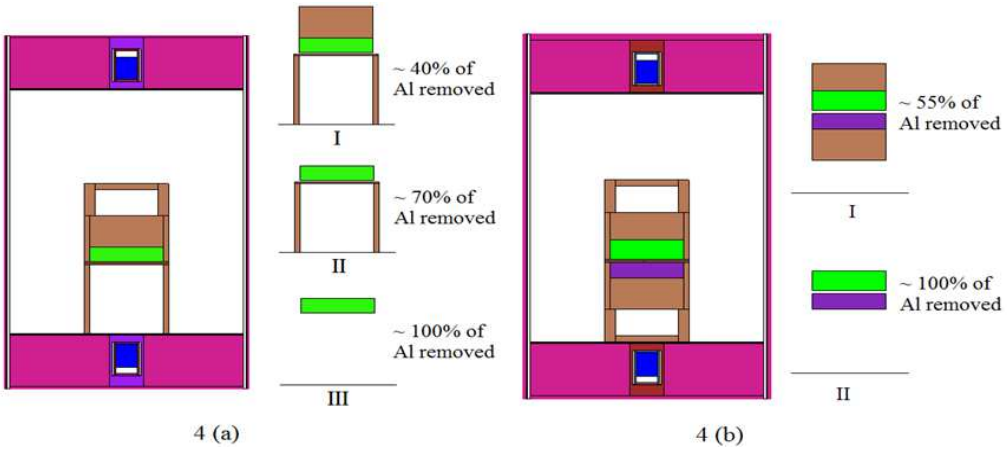

Fig. (4). *Geometrical model of the AWCC used for Monte Carlo calculations for different setup configurations of Al parts with (a) single and (b) coupled NM samples.*

To investigate the Al attenuation affects the thermal neutron (resulting from AmLi neutrons thermalized by the polyethylene) and/or the fast neutrons (resulting from 235U fission neutrons), the percentage of neutron current attenuated by Al with three different thicknesses (1.0, 2.0 and 5.0 cm) as a function of the incident neutron energy beam was studied with MCNP code. The assumed neutron source is a point source emits mono-energetic and mono-directional neutrons with energies of 0.001, 0.01, 0.1, 0.2, 0.3, 0.45, 0.7, 1.0, 1.98, 5.0 and 10.0 MeV. The mean energy values for the Am Li neutrons (0.45 MeV) and 235U fission neutrons (1.98 Mev) were considered. The neutron source was assumed to be perpendicular to and 1.0 cm away from the outer surface of the Aluminum cell.

The second factor that was expected to be a main source of error is the pressure of 3He detectors. The information provided by the manufacture does not allow accurate simulation of the detectors. To study the effect of 3He pressure, the atom density of the gas was changed in the MC input files to be 50%, 75%, 150% and 200% of the expected density.

The main bulk of the AWCC counter body is made of polyethylene (the moderator). Any small change in its density was expected also to be a source of error. The polyethylene density was used in two different values, 0.955 and 0.97 g/cm3 [30, 31]. This variation in densities was also studied.

Although the samples assayed in the AWCC are measured in 4π-configuration, the location of the sample inside the cavity of the counter (or the cavity height itself) could affect the response of the counter. If it is not determined accurately, it may contribute to the overall error. This is due to the fact that the neutron flux is not uniformly distributed inside the cavity along both the axial and radial directions.

Polyethylene is containing hydrogen which thermalizes neutrons, so it will be essential to use Thermal S(α,β) Cross-Section Libraries to get correct results in such problems [33]. This treatment takes into account how a collision between a neutron and an atom is affected by the thermal motion of the atom and the presence of other atoms nearby- in other words, it takes into account the scattering of neutrons at low

(thermal) energy in a moderator [34]. In our case, two different S(α,β) cross-section libraries could be appropriate for neutrons transport in polyethylene; poly.01t and poly.60t. Information about S(α,β) data for these two codes is contained in the following table [33].

Table 3. *The main information for S(α,β) cross-section libraries of poly.01t and poly.60t codes.*

ZAID	Source	Library name	Temp (K°)	No. of Angles	No. of Energies	Elastic Data
poly.01t	endf5	Tmccs	300	8	20	Inco
poly.60t	endf6.3	sab2002	294	16	64	Inco

Where;

Temperature: is the temperature of the data in degrees Kelvin.

Number of Angles: is the number of equally-likely discrete secondary cosines provided at each combination of incident and secondary energy for inelastic scattering and for each incident energy for incoherent elastic scattering.

Number of Energies: is the number of secondary energies provided for each incident energy for inelastic scattering.

Elastic Data: for (inco); it is incoherent elastic scattering data provided for this material.

Poly.01t and poly.60t cross-section libraries in addition to the running of the input files without poly.t cross-section library were examined to determine the suitable one for the MC calculations in case of AWCC neutron coincidence counting.

4. Results and Discussion

4.1. Measured and Calculated Coincidence Count Rates

The AWCC was mathematically modeled using the MCNP code. The information used for constructing the MCNP input file was obtained mainly from the manufacturer, while other – not provided by the manufacturer - was obtained from literature. The results obtained from the model (real coincidence count rates, C_{r5}) were compared with measurements to check the accuracy of the model. Tables (4) and (5) give the obtained results for the measured and modeled coincidence count rates, for single and coupled NM samples, respectively.

Table (4) shows that the relative accuracy of the model ranges between 7.37% for SRM-071 to -6.15% for SRM-295 for single NM samples. For the coupled samples, relative accuracy ranges between 8.46% for SRM-071+071 and -2.08% for SRM-446+071, Table 5.

Table 4. *Results of measured and calculated C_{r5} for single NM sample with associated accuracy.*

SNM ID	^{235}U weight, g	Measured C_{r5}, $s^{-1} \pm \sigma$	Simulated C_{r5}, s^{-1}	Accuracy %
SRM-071	1.2047	28.5 ± 0.32	26.40	7.37
SRM-194	3.2918	71.8 ± 0.51	71.93	-0.18
SRM-295	5.0056	100.3 ± 0.51	106.47	-6.15
SRM-446	7.5678	138.0 ± 1.20	144.63	-4.80

Table 5. *Results of measured and calculated C_{r5} for coupled NM samples with associated accuracy.*

SNM ID	^{235}U weight, g	Measured C_{r5}, $s^{-1} \pm \sigma$	Simulated C_{r5}, s^{-1}	Accuracy %
SRM-071+071	2.4094	55.2 ± 0.22	50.53	8.46
SRM-071+194	4.4965	97.7 ± 0.32	92.82	4.99
SRM-071+295	6.2103	126.8 ± 0.41	125.17	1.28
SRM-446+031	8.0938	146.5 ± 1.01	144.68	1.24
SRM-446+071	8.7725	159.9 ± 0.71	163.23	-2.08
SRM-446+194	10.8596	197.5 ± 0.32	198.71	-0.61
SRM-446+295	12.5734	221.5 ± 0.81	225.06	-1.61
SRM-446+446	15.1355	250.0 ± 0.51	254.75	-1.90

The trend of the obtained results could be understood keeping in mind that the AWCC is basically designed for assaying samples with relatively large masses and with a minimum detection limit of 1g ^{235}U [25]. It is clear from both tables that as the ^{235}U mass increased the estimated accuracy is improved as a result of improvement of statistic, except for some cases in which single NM samples were measured and also in which the natural uranium sample was involved. It is clear from the tables also that, to some extent, the accuracy is a function of the volume distribution of the sample inside the cavity of the counter. Although sharp conclusions could not be drawn for such small ^{235}U masses, still the sources of errors could be investigated aiming at well understanding of their effects on the model in addition to improvement of the estimated accuracy. In the following the evaluation of expected sources of errors is presented.

4.2. Different Factors Affecting the MC Modeling

In the following, different factors affecting the calculations are presented. The calculated accuracies are given for each

case beside the original accuracy values (i.e., the accuracy before considering the effect, mentioned as "None").

4.2.1. Al container and Holder Effect

Tables (6) and (7), show that by removing some parts of the Al container and holder, the values of C_{r5} increases for both single and coupled NM calculations, meaning that there is an attenuation effect resulting from the Al components. It is clear also that the attenuation effect is relatively large. The removal of the outer Al container (Table (7), column I) resulted in a difference in C_{r5} of about 3% from the original value for the coupled samples. This considerable change reflects the importance of accurate and detailed information while creating the MCNP input file.

Table 6. *Measured and calculated C_{r5} for single NM samples and the effect of Al parts removal on calculations. The removed parts (I, II and III) are as illustrated in figure 4(a).*

SNM ID	^{235}U weight, g	Measured C_{r5}, $s^{-1} \pm \sigma$	Simulated C_{r5}, s^{-1}	Accuracy% Al Parts removed			
				None*	I	II	III
SRM-071	1.2047	28.5 ± 0.32	26.40	7.37	-0.56	-7.19	-22.74
SRM-194	3.2918	71.8 ± 0.51	71.93	-0.18	-4.37	-9.94	-15.13
SRM-295	5.0056	100.3 ± 0.51	106.47	-6.15	-6.38	-11.17	-15.68
SRM-446	7.5678	138.0 ± 1.20	144.63	-4.80	-6.96	-13.7	-14.78

Table 7. *Measured and calculated C_{r5} for coupled NM samples and the effect of Al parts removal on calculations. The removed parts (I and II) are as illustrated in figure 4(b).*

SNM ID	^{235}U weight, g	Measured C_{r5}, $s^{-1} \pm \sigma$	Simulated C_{r5}, s^{-1}	Accuracy % Al Parts removed		
				None	I	II
SRM-071+071	2.4094	55.2 ± 0.22	50.53	8.46	5.71	-8.32
SRM-071+194	4.4965	97.7 ± 0.32	92.82	4.99	3.53	-8.22
SRM-071+295	6.2103	126.8 ± 0.41	125.17	1.29	1.17	-11.77
SRM-446+031	8.0938	146.5 ± 1.01	144.68	1.24	-3.78	-10.45
SRM-446+071	8.7725	159.9 ± 0.71	163.23	-2.08	-4.60	-11.63
SRM-446+194	10.8596	197.5 ± 0.32	198.71	-0.61	-3.69	-10.92
SRM-446+295	12.5734	221.5 ± 0.81	225.06	-1.61	-4.47	-11.45
SRM-446+446	15.1355	250.0 ± 0.51	254.75	-1.90	-5.15	-10.56

The attenuation effect of Al was studied with MCNP code. Figure (5), shows the attenuation of an incident neutron current on different thicknesses of Al strips (1.0, 2.0 and 5.0 cm) as a function of its energy. It is clear that the neutron current is attenuated with different percentages depending on the incident neutron energy beam, the Al thickness and whether they are thermal or fast neutrons. In case of 1.0 cm of Al thickness the neutron current attenuation increases rapidly from about 3.75% at thermal neutrons to be about 11.5% at 0.3 MeV, then decreases to 3.8 at 1.0 MeV. For the wide range of energies varies from 1.0 to 10.0 MeV, the attenuation ratio approximately unchanged (about 4.0% from the initial value).

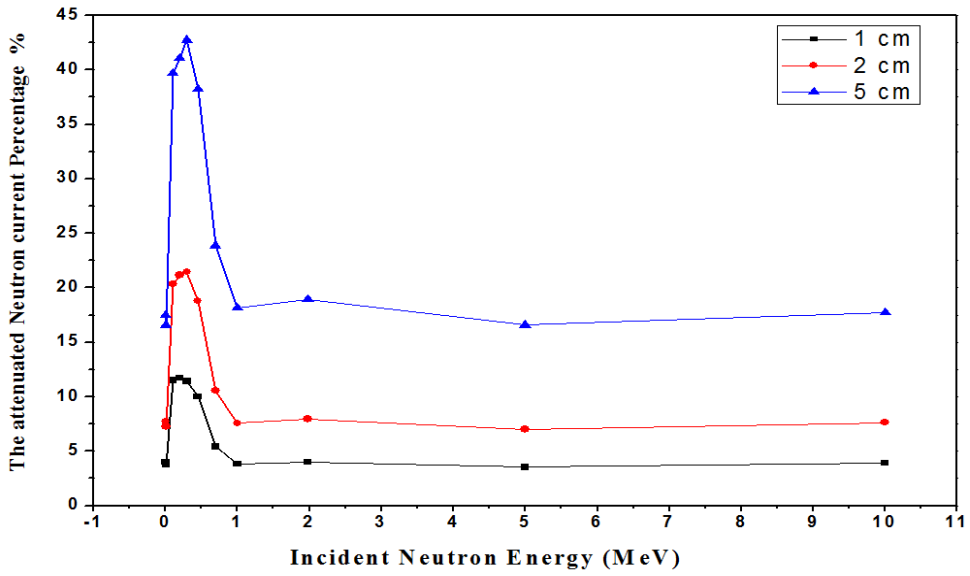

Fig. (5). *Percentage of neutron current attenuated as a function of the incident neutron energy beam in three suggested Al thicknesses.*

From these calculations it is clear that the information about materials of container and holder, their shapes, configurations and locations inside the cavity of the counter are essential factors in this type of calculations.

4.2.2. ^{3}He Pressure Effect

Tables (8) and (9), show that by changing the density of ^{3}He the values of C_{r5} changes accordingly for both single and coupled NM calculations. For example the decreasing of ^{3}He density to become 75% of its assumed original value resulted in a decreasing in C_{r5} of about 5 to 7% for single samples and about 4 to 6.5% for coupled samples from the original value. On the other hand increasing the density to become 150% resulted in an increase of C_{r5} by about 2 to 6% for single samples and about 5.25 to 7.5% for coupled samples from its original value.

Table 8. *Measured and calculated C_{r5} for single NM samples and the effect of changing the ^{3}He density to be 50%, 75%, 150% and 200%.*

SNM ID	^{235}U weight, g	Measured C_{r5}, $s^{-1} \pm \sigma$	Simulated C_{r5}, s^{-1}	Accuracy %				
				Relative changing of ^{3}He density (ρ =)				
				None	50 %	75%	150 %	200 %
SRM-071	1.2047	28.5 ± 0.32	26.40	7.37	32.07	14.37	5.52	-0.08
SRM-194	3.2918	71.8 ± 0.51	71.93	-0.18	17.84	4.77	-6.28	-10.88
SRM-295	5.0056	100.3 ± 0.51	106.47	-6.15	12.28	0.76	-11.36	-15.71
SRM-446	7.5678	138.0 ± 1.20	144.63	-4.80	11.59	1.08	-11.75	-15.87

Table 9. *Measured and calculated C_{r5} for coupled NM samples and the effect of changing the ^{3}He density to be 50%, 75%, 150% and 200%.*

SNM ID	^{235}U weight, g	Measured C_{r5}, $s^{-1} \pm \sigma$	Simulated C_{r5}, s^{-1}	Accuracy %				
				Relative changing of ^{3}He density (ρ =)				
				None	50 %	75%	150 %	200 %
SRM-071+071	2.4094	55.2 ± 0.22	50.53	8.46	29.16	12.40	3.21	-1.82
SRM-071+194	4.4965	97.7 ± 0.32	92.82	4.99	22.06	11.38	-1.84	-5.23
SRM-071+295	6.2103	126.8 ± 0.41	125.17	1.29	18.75	7.52	-5.74	-8.99
SRM-446+031	8.0938	146.5 ± 1.01	144.68	1.24	17.82	7.34	-5.84	-9.17
SRM-446+071	8.7725	159.9 ± 0.71	163.23	-2.08	15.32	4.66	-9.21	-12.93
SRM-446+194	10.8596	197.5 ± 0.32	198.71	-0.61	16.32	5.54	-8.15	-11.24
SRM-446+295	12.5734	221.5 ± 0.81	225.06	-1.61	15.05	4.63	-8.91	-12.34
SRM-446+446	15.1355	250.0 ± 0.51	254.75	-1.90	14.83	4.60	-9.38	-13.98

4.2.3. Polyethylene EFFECT

Tables (10) and (11), show the effect of changing some parameters related to polyethylene in MCNP input files; For polyethylene density to become 0.97 g/cm^3 instead of the used density 0.955 g/cm^3 in our input files, it shows that similar accuracy results were obtained for both of them, however the overall standard deviation and the mean value related to the accuracy results in case of ρ= 0.955 g/cm^3 were relatively more acceptable and reliable than the estimated results with ρ= 0.97 g/cm^3. Table (12), shows the main statistics related to the overall accuracy values given in (Tables 10 and 11), including the standard deviations and the mean values for; none, a, b and c cases.

In case of using MCNP poly.60t cross-section library instead of the used poly.01t, the fluctuations were large. Table (12), clarify also that the standard deviation and the mean value related to the accuracy results in this case were poor. When the input files used without poly.t cross-section library, the fluctuations were extremely very large and the standard deviation and the mean value related to it were unacceptable and unreliable.

Table 10. *Measured and calculated C_{r5} for single NM samples in a comparison with the resulted data of changing some parameters related to polyethylene in MCNP input files: (a) polyethylene density to be 0.97 g/cm^3 instead of the used density 0.955 g/cm^3 (b) with poly.60t cross-section library instead of the used poly.01t (c) without poly.t cross-section library.*

SNM ID	^{235}U weight, g	Measured C_{r5}, $s^{-1} \pm \sigma$	Simulated C_{r5}, s^{-1}	Accuracy %			
				Diff Parameters effect			
				None	(a)	(b)	(c)
SRM-071	1.2047	28.5 ± 0.32	26.40	7.37	8.67	10.43	134.80
SRM-194	3.2918	71.8 ± 0.51	71.93	-0.18	-3.89	-0.75	44.95
SRM-295	5.0056	100.3 ± 0.51	106.47	-6.15	-7.93	-7.13	37.73
SRM-446	7.5678	138.0 ± 1.20	144.63	-4.80	-6.74	-5.72	29.52

Table 11. *Measured and calculated C_{r5} for coupled NM samples in a comparison with the resulted data of changing some parameters related to polyethylene in MCNP input files: (a) polyethylene density to be 0.97 g/cm^3 instead of the used density 0.955 g/cm^3 (b) with poly.60t cross-section library instead of the used poly.01t (c) without poly.t cross-section library.*

SNM ID	^{235}U weight, g	Measured C_{r5}, $s^{-1} \pm \sigma$	Simulated C_{r5}, s^{-1}	Accuracy %			
				Diff Parameters effect			
				None	(a)	(b)	(c)
SRM-071+071	2.4094	55.2 ± 0.22	50.53	8.46	7.74	26.28	159.47
SRM-071+194	4.4965	97.7 ± 0.32	92.82	4.99	2.73	10.94	76.27
SRM-071+295	6.2103	126.8 ± 0.41	125.17	1.29	-0.06	5.53	57.30
SRM-446+031	8.0938	146.5 ± 1.01	144.68	1.24	1.32	0.96	51.94
SRM-446+071	8.7725	159.9 ± 0.71	163.23	-2.08	-1.37	-0.42	47.25
SRM-446+194	10.8596	197.5 ± 0.32	198.71	-0.61	-1.12	-0.08	44.85
SRM-446+295	12.5734	221.5 ± 0.81	225.06	-1.61	-2.53	-1.10	39.72
SRM-446+446	15.1355	250.0 ± 0.51	254.75	-1.90	-2.13	-0.22	36.54

Table 12. *The main statistics related to the overall accuracy values given in table 10 and 11.*

Related Parameter	Mean	SD	Minimum	Median	Maximum
None	0.50	4.50	-6.15	-0.39	8.46
(a)	-0.68	5.01	-8.61	-1.26	7.98
(b)	2.50	7.81	-7.68	-0.15	20.81
(c)	36.01	12.13	22.79	31.55	61.46

5. Conclusion

Monte Carlo simulation model for calibration of the AWCC has been proposed and verified using sets of SNM samples contains small ^{235}U masses. The obtained modeling results are found to be in agreement with experiments within an accuracy of better than 8.5%. As ^{235}U mass increased the estimated accuracy is improved due to the improvement of statistics. The expected sources of errors related to the precise determination of the counter and/or experimental set up parameters has been studied, aiming to be understand well their effects on the model in addition to improve the estimated accuracy. More investigations are still needed to improve the accuracy of the proposed method. The proposed method could be employed to overcome the lack of NM standards needed (that would be difficult and expensive) for the detector calibration.

References

[1] W. El-Gammal, W. I. Zidan and E Elhakim. A proposed semi-empirical method for ^{235}U mass calibration of the active-well neutron coincidence counter. Nuclear Instruments and Methods A565 (2006) 731.

[2] H.O. Menlove, Description and operation manual for the active well coincidence counter, LA-7823-M, Los Alamos, 1979.

[3] H.O. Menlove and J.E. Swansen, Nucl. Technol. 71 (1985) 497.

[4] J.E. Swansen, P.R. Collinsworth and M.S. Krick, Nucl. Instr. and Meth. 176 (1980) 555.

[5] M.M. Stephens, J.E. Swansen and L.V. East, Shift register neutron coincidence module, LA-6121-MS, Los Alamos, 1975.

[6] M.S. Krick, N. Ensslin, D. G. Langner, M. C. Miller, R. Siebelist, and J. E. Stewart, Active Neutron Multiplicity Analysis and Monte Carlo Calculations, Institute of Nuclear Materials Management (INMM), Florida, USA, July 17-20, 1994.

[7] H.O. Menlove, N. Ensslin and T.E. Sampson, Experimental comparison of the active well coincidence counter with the random driver, LA- 7882-MS, Los Alamos, 1979.

[8] R. Sher, Active neutron coincidence counting for the assay of MTR fuel elements, LA-9665-MS, Los Alamos, 1983.

[9] H.O. Menlove and G.E. Bosler, Application of the active well coincidence counter (AWCC) to high-enrichment uranium metal, LA-8621-MS, Los Alamos, 1981.

[10] M.S. Krick, H.O. Menlove, J. Zick and P. Ikonomou, Measurement of enriched uranium and uranium-aluminum fuel materials with the AWCC, LA-10382-MS, Los Alamos, 1985.

[11] M.S. Krick and P.M. Rinard, Field tests and evaluations of the IAEA active-well coincidence counter, LA-9608-MS Los Alamos, 1982.

[12] W.G. Winn and E.T. Booth, Nucl. Inst. and Meth. 200 (2/3) (1982) 597.

[13] J.K. Hartwell and G.D. McLaughlin, Non-destructive analysis of impure HEU-carbon samples using an active well coincidence counter (AWCC) 39, in: INMM Annual Meeting, Naples, FL, USA, 26–30, July 1998.

[14] V. Mykhaylov, M. Odeychuk, V. Tovkanetz, V. Lapshyn, K. Thompson and J. Leicman, Use of AWCC in evaluation of unknown fissile materials, in: Symposium on International Safeguards: Verification and Nuclear Material Security, IAEA-SM-367, Vienna, Austria, 29 October - 2 November 2001.

[15] B.A. Jensen, J. Sanders, T. Wenz and R. Buchheit, Results of active well coincidence counter cross-calibration measurements at Argonne National Laboratory-West, ANL-02/35, Argonne, 2002.

[16] H.O. Menlove, R. Siebelist and T.R. Wenz, Calibration and performance testing of the IAEA Aquila active well coincidence counter (Unit 1), LA-13073-MS, Los Alamos, 1996.

[17] H.O. Menlove and J.E. Stewart, A new method of calibration and normalization for neutron detector families, LA-11229-MS, Los Alamos, 1988.

[18] P. Rinard and H. Menlove, Monte Carlo simulations of an AWCC with long fuel assemblies, in: Symposium on Safeguards and Nuclear Material Management, Seville, Spain, 4–5 May 1999.

[19] Sara A. Pozzi, Richard B. Oberer, and Lisa G. Chiang, Monte Carlo Simulation of Measurements with an Active Well Coincidence counter, Oak Ridge National Laboratory available on "http://www.ornl.gov/~webworks/cppr/y2001 /pres/120718.pdf".

[20] T. D. Reilly, N. Ensslin, H. A. Smith and S. Kreiner, "Passive Nondestructive Assay of Nuclear Materials," NUREG/CR-5550, LA-UR-90-732, Los Alamos National Laboratory (USA), 1991.

[21] N. Ensslin, W.C. Harker, M.S. Krick, D.G. Langner, M.M. Pickrell and J.E. Stewart, Application Guide to neutron multiplicity counting, LA-13422-M, Los Alamos, 1998.

[22] D.I. Garber and R.R. Kinsey, Neutron Cross Sections, vol. II, Curves, BNL 325, Brookhaven National Laboratory, 1976.

[23] M. Ebied, M.Sc Thesis, Investigation of Depleted Uranium Assay using Active Well Neutron Coincidence Counter, Physics Department, Faculty of Science, Al-Azhar University, April 2009.

[24] H. Tagziria and M. Looman, The ideal neutron energy spectrum of ^{241}AmLi (α,n) 10B sources, Applied Radiation and Isotopes 70 (2012) 2395.

[25] CANBERRA, Model JCC-51, Active well neutron coincidence counter, User's Manual, USA, 1998.

[26] CANBERRA, Neutron coincidence counter checklist, ^{3}He Tube Data Sheets, USA, 1998.

[27] CANBERRA, Model JSR-14, Neutron analysis shift register, User's Manual, USA, 1997.

[28] National Bureau of Standards Certificate. Standard Reference Material 969: Uranium isotopic standard reference material for gamma spectrometry measurement. (In cooperation with the Commission of the European Communities, Central Bureau for Nuclear Measurements, Geel, Belgium, and the U.S. Department of Energy, New Brunswick Laboratory, Argonne, Illinois) Gaithersburg, USA, MD 20899 (October 15, 1985) Revision dated July 27, 1985.

[29] S. Croft, E. Alvarez, R. D. McElroy and C. G. Wilkins, the Absolute Calibration of Active Neutron Assay Instruments, Neutron Waste Management and Special Systems – Technical Papers, Canberra Industries, available on "http://www. canberra.com/literature/waste_special_systems/tech_papers/A ctiveNeutronAssay-paper.pdf"

[30] Eric Chandler Miller, Characterization of Fissionable Material using a Time-Correlated Pulse-Height Technique for Liquid Scintillators, a dissertation submitted in partial fulfillment of the requirements for the degree of Doctor of Philosophy, Nuclear Engineering and Radiological Sciences, University of Michigan, 2012.

[31] Corey Freeman, William Geist and Martyn Swinhoe, MCNPX Calculations of MTR Fuel Elements Measured in an Active Well Coincidence Counter, LA-UR-09-03916, Los Alamos, June 2009.

[32] X-5 Monte Carlo Team, MCNP - A General Monte Carlo N-Particle Transport Code, Version 5, Volume II: User's Guide, LA-CP-03-0245 (Revised 10/3/05), April 24, 2003.

[33] X-5 Monte Carlo Team, MCNP - A General Monte Carlo N-Particle Transport Code, Version 5, Volume I: Overview and Theory, LA-UR-03-1987 (Revised 10/3/05), April 24, 2003.

[34] Alexis Lazarine Reed, Medical Physics Calculations with MCNP: A primer, Los Alamos National Laboratory, LA-UR-07-4133, Summer American Nuclear Society Meeting, Boston, June 25-28, 2007.